A Journal of the Gesellschaft Deutscher Chemiker

Angewandte International Edition Chemie

GDCh

www.angewandte.org

Accepted Article

Title: Insights into desaturation of cyclopeptin and its C3-epimer catalyzed by a non-heme iron enzyme: structural characterization and mechanism elucidation

Authors: WEI-CHEN CHANG, Hsuan-Jen Liao, Jikun Li, Jhih-Liang Huang, Madison Davidson, Igor Kurnikov, Te-Sheng Lin, Justin L. Lee, Maria Kurnikova, Yisong Guo, and Nei-Li Chan

To be cited as: *Angew. Chem. Int. Ed.* 10.1002/anie.201710567
Angew. Chem. 10.1002/ange.201710567

Link to VoR: http://dx.doi.org/10.1002/anie.201710567
http://dx.doi.org/10.1002/ange.201710567

WILEY-VCH

10.1002/anie.201710567

WILEY-VCH

COMMUNICATION

Insights into desaturation of cyclopeptin and its C3-epimer catalyzed by a non-heme iron enzyme: structural characterization and mechanism elucidation

Hsuan-Jen Liao,[c]† Jikun Li,[b]† Jhih-Liang Huang,[a] Madison Davidson,[a] Igor Kurnikov,[b] Te-Sheng Lin,[c] Justin L. Lee,[b] Maria Kurnikova,[b]* Yisong Guo,[b]* Nei-Li Chan,[c]* and Wei-chen Chang[a]*

Abstract: AsqJ, an iron(II) and 2-oxoglutarate dependent enzyme found in viridicatin-type alkaloid biosynthetic pathways, catalyzes sequential desaturation and epoxidation to produce cyclopenins. Herein, the crystal structures of AsqJ bound to cyclopeptin and its C3-epimer are reported. Meanwhile, a detailed mechanistic study was carried out to provide compelling evidence in deciphering the desaturation mechanism. These findings suggest that a pathway involving hydrogen atom abstraction at the C10 position of the substrate by a short-lived Fe(IV)-oxo species and the subsequent formation of a carbocation or a hydroxylated intermediate is likely to be utilized during AsqJ catalyzed desaturation.

AsqJ, an iron(II) and 2-oxogluatrate (Fe/2OG) enzyme, has recently been discovered in viridicatin-type alkaloid biosynthesis in *Aspergillus nidulans*. It catalyzes two consecutive reactions: a C=C bond formation and an epoxidation to enable formation of the 6,6-bicyclic core of the viridicatin scaffold (Scheme 1A)[1]. Recently, we and other research groups have presented a plausible mechanism for the epoxidation catalyzed by AsqJ[1-2]. However, mechanistic understanding of AsqJ-catalyzed desaturation has not been elucidated.

In general, two approaches have been utilized by biological systems to construct C=C bonds. One involves introduction of a leaving group followed by β-elimination. The other approach involves a direct C-H bond activation process where metal-cofactors, such as heme-iron centers, non-heme mono-iron centers, or di-iron centers, are required to trigger the reaction[3]. For two mechanistically characterized desaturases, fatty acyl desaturases and cytochrome P-450 enzymes (Scheme 1B), enzymatic and biomimetic model studies support a mechanism involving two consecutive hydrogen atom transfer processes (2-HAT) to construct a C=C bond[3a-c, 3e, 3j]. Specifically, a di-(μ-oxo)-di-iron(IV/IV) intermediate or a ferryl porphyrin radical cation species, compound I, functions as the key intermediate to trigger the first C-H bond cleavage, and a proposed Fe_2(III/IV) intermediate or an Fe(IV)-hydroxo complex, compound II, is hypothesized to serve as the second hydrogen atom (H•) abstractor to produce a di-radical species prior to C=C bond formation. In both cases, the initial reactive species stores two potent oxidizing equivalents for sequential C-H bond activation. It should be noted that an alternative mechanism involving a cation intermediate has also been proposed in P-450 desaturases[3d, 3g]. Similarly, an analogous 2-HAT mechanism has been suggested in Fe/2OG enzyme catalyzed desaturation, such as in flavone synthase I, carbapenem synthase, and clavaminate synthase[3f, 3h, 3i, 3k]. Compared to the well-studied hydroxylation mechanism[4] where the reaction proceeds through H• abstraction by an Fe(IV)=O species followed by formation of a C-O bond between the substrate radical and the Fe(III)-OH intermediate, during the desaturation, the resulting Fe(III)-OH intermediate is used as the second H• abstractor to produce a di-radical intermediate (Scheme 2B). Inspired by recent discovery of Fe/2OG enzyme catalysis[4], pathways involving a carbocation or a hydroxylated intermediate generated after the incipient C-H bond activation also need to be considered (Scheme 2B). Herein, we use a complementary approach consisting of probe design, X-ray crystallography, stopped-flow optical absorption, freeze quench coupled Mössbauer spectroscopy, MD simulations and MS-based product analysis to elucidate desaturation mechanism. Our results suggest that AsqJ catalyzed desaturation is likely to initiate from C10-H abstraction by a short-lived Fe(IV)-oxo species. The reaction is likely followed by formation of a carbocation or a hydroxylated intermediate to complete installation of C=C bond.

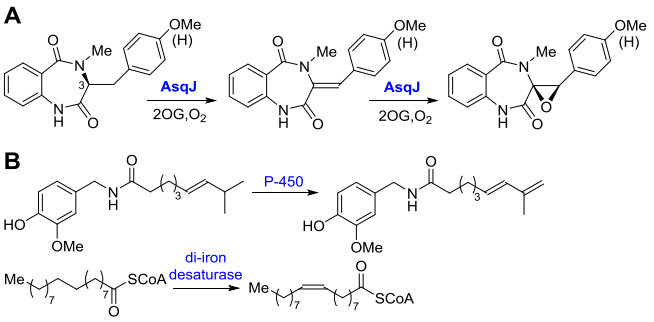

Scheme 1. (A). AsqJ catalyzed consecutive desaturation and epoxidation. (B) Examples of desaturation catalyzed by cytochrome P-450 and di-iron cofactors containing enzymes.

[a] J.-L. Huang, M. Davidson, Prof. W.-c. Chang
Department of Chemistry, North Carolina State University
Raleigh, NC 27695, U.S.A.
E-mail: wchang6@ncsu.edu
[b] J. Li, I. Kurnikov, J. L. Lee, Prof. M. Kurnikova, Prof. Y. Guo
Department of Chemistry, Carnegie Mellon University
Pittsburgh, PA 15213, U.S.A.
E-mail: ysguo@andrew.cmu.edu & kurnikova@cmu.edu
[c] H.-J. Liao. T.-S. Lin, Prof. N.-L. Chan
Institute of Biochemistry and Molecular Biology, College of Medicine,
National Taiwan University, Taipei 100, Taiwan
E-mail: nlchan@ntu.edu.tw
Supporting information for this article is given via a link at the end of the document.

10.1002/anie.201710567

WILEY-VCH

COMMUNICATION

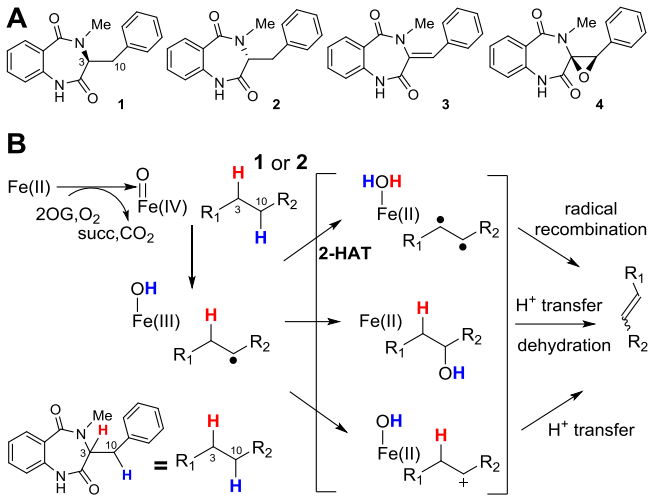

Scheme 2. (A) Mechanistic probes and AsqJ reaction products used in this study. (B) Proposed pathways accounting for AsqJ catalzyed desaturation. After C10-H activation, the reaction can proceed through (i) second hydrogen atom abstraction (2-HAT) and followed by di-radical recombination, (ii) hydroxylation and dehydration, or (iii) a carbocation formation and subsequent H^+ removal to complete the C=C bond installation.

To probe the potential mechanism of AsqJ catalyzed desaturation, cyclopeptin (**1**), its C3-stereoisomer (**2**), and products (**3**) and (**4**) were prepared (Scheme 2A)[2b, 5]. To examine the suitability of **2** as a mechanistic probe, we solved the crystal structures of AsqJ•Fe•2OG•**1** and AsqJ•Fe•2OG•**2** complexes at 1.96 and 2.05 Å resolution by molecular replacement using the published substrate bound AsqJ structure (AsqJ•Ni•2OG•**1** complex)[2a] as the search model (PDB: 5Y7R, 5Y7T) (Table S1). In contrast to the published structures where the Fe was replaced by Ni during protein purification[2a], the two structures reported herein represent the first visualization of AsqJ in its native Fe-bound forms. An XANES spectrum collected from an AsqJ•Fe•2OG•**1** crystal unambiguously shows the presence of iron in the crystal (Fig. S4). The structure of AsqJ•Fe•2OG•**1** closely resembles the structure of AsqJ•Ni•2OG•**1** (Fig. S5)[2a]. Importantly, **1** and **2** bound AsqJ structures are also highly similar. In both structures, the benzodiazepinedione, the phenyl group, and both C3, and C10 centers are well defined in the electron density maps (Fig. 1, S6 and S7). The phenyl ring of **1** or **2** is stabilized by van der Waals interactions with residues V72, L79, M118, and F139, along with plausible π-π interaction with H134 (Figure S6). The change of chirality at the C3 position does however cause structural flipping of C10 and a subtle reposition of the phenyl group (Fig. 1C). Compared to the distances of C10 and C3 of **1** to the iron center (4.8 and 4.5 Å), the corresponding distances in **2** are 3.7 and 4.9 Å, respectively (Fig. 1D). More importantly, different from the binding configuration of **1** where the C3-H and one of the C10-Hs are poised toward the iron center, in the structure of AsqJ•Fe•2OG•**2**, the C3-H points away from the iron center and only one of the C10-Hs is poised toward it. These structures clearly demonstrate that **1** and its C3-epimer (**2**) bind analogously to the active site of AsqJ. Furthermore, It implicates the plausibility of using **2** to probe the desaturation mechanism. We hypothesize that the reaction is likely to initiate from C10-H abstraction. Subsequently, if a second H• abstraction is required to complete desaturation, the use of **2** will abolish the C3-H• abstraction and may lead to the acculumation of the substrate radical species or redirect the reaction outcome from desaturation to hydroxylation. In contrast, if **2** can be converted to **3**, other posssible pathway(s) which involve either a carbocation or a hydroxylated intermediate would need to be considered.

To support that the substrate binding modes obtained from our crystallographic data are energetically stable in solution, we conducted molecular dynamics (MD) simulations on the available crystal structures of AsqJ. MD simulations in combination of QM/MM calculations have been previously used to elucidate Fe/2OG enzyme catalyzed chlorination, desaturation and epoxidation mechanisms[6]. Using the published AsqJ•Ni(II)•**1**•2OG structure (PDB: 5DAW) as the starting point with the replacement of Ni(II) to Fe(II), MD equilibrated structure of the AsqJ•Fe(II)•2OG•**1** complex resembles closely to the crystal structure described above (Fig. S8). Furthermore, in accordance with the crystal structure of AsqJ•Fe•2OG•**2** complex, the MD simulation predicted binding configuration of **2** is similar to that of **1**, except that the C3-H points away from the iron center (Fig. S8 and S10). In addition, MBAR computed the binding free energy difference between **1** and **2** as ~0.4 kcal/mol with **1** having slightly tighter binding to AsqJ (Fig. S9). Thus, both experimentally determined and computationally simulated structures reveal the highly similar binding configurations of **1** and **2** to AsqJ.

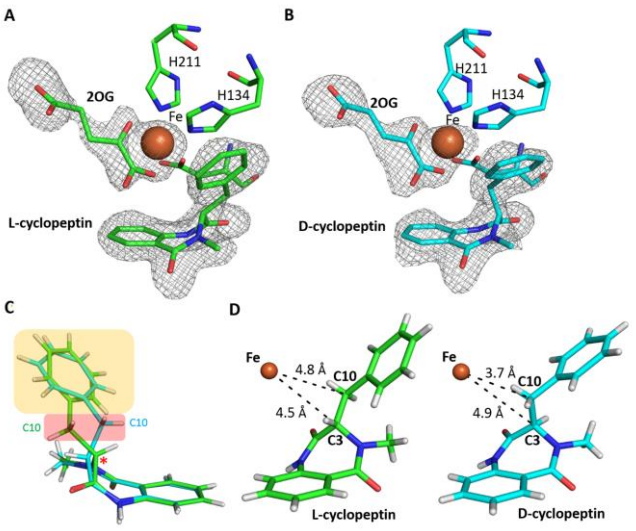

Figure 1. Crystal structures of the AsqJ•Fe•2OG•**1** and AsqJ•Fe•2OG•**2**. (A) and (B) Close-up views of the AsqJ active site. The *Fo-Fc* electron density maps are shown in grey mesh and contoured at 2.8 σ. The bound 2OG, **1** (panel A) or **2** (panel B), and the Fe-ligating residues are shown in stick form. The Fe is shown as orange sphere. The carbon atoms of 2OG, substrate, and selected amino acid side chains are colored green (for AsqJ•Fe•2OG•**1**) or cyan (for AsqJ•Fe•2OG•**2**). The remaining atoms (nitrogen, oxygen, sulfur) in both structures are colored according to the CPK scheme. (C) Alteration of the stereochemistry at the C3 (red asterisk) repositions the C3-hydrogen, C10 (red shaded), and the phenyl group (brown shaded) of **2** (cyan) relative to **1** (green). (D) The Fe-C3 and Fe-C10 distances observed in the **1** (left) and **2** (right) bound AsqJ structures. (PDB: 5Y7R, 5Y7T).

10.1002/anie.201710567

Next, we conducted stopped-flow optical absorption (SF-Abs) measurements to reveal the effect of **1** and **2** on AsqJ reaction kinetics. The SF-Abs experiment was carried out by rapidly mixing an anaerobic solution containing the AsqJ•Fe(II)•2OG•subtrate complex (AsqJ 0.5 mM, Fe(II) 0.4 mM, 2OG 4.0 mM, and **1** or **2** 0.4 mM) with air-saturated buffer (~0.4 mM of O_2). The SF-Abs spectra showed a very similar kinetic behavior of the absorption feature centered ~470 nm when either **1** or **2** was used (Fig. 2). This feature represents the metal-to-ligand charge transfer (MLCT) band of the Fe(II)-2OG complex[7] and similar decay kinetics suggests that both **1** and **2** can trigger 2OG consumption with similar efficacy. In addition, a simultaneous increase of absorption at ~310 nm was observed (Fig. 2, S15). In characterized Fe/2OG enzymes[8], the absorbance change at ~310 nm is attributed to the accumulation of an Fe(IV)-oxo intermediate. However, based on Mössbauer and LC-MS results (see below), the absorbance change at ~310nm likely represented formation of **3**. The highly similar kinetic behavior of **1** and **2** implies that the C3 chirality is not critical for the reaction.

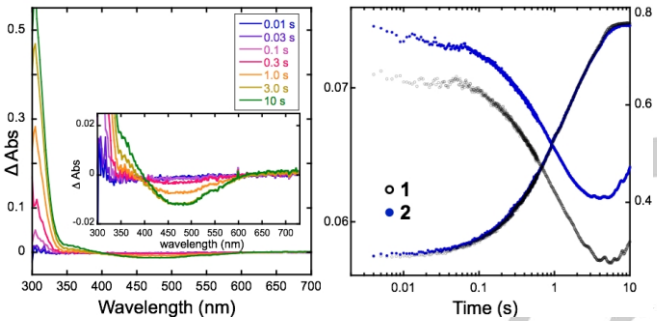

Figure 2. SF-Abs kinetics of AsqJ catalyzed reactions by using **1** or **2**. Left: Absorption changes at the indicated reactions times after mixing anaerobic AsqJ•Fe(II)•2OG•**1** complex with O_2 (inset: absorption changes centered at 470 nm). Right: The decay of Fe(II)-2OG MLCT band at 470 nm (left vertical axis) and the increase of the absorption at ~310 nm (right vertical axis) in the reaction of the AsqJ•Fe(II)•2OG•substrate complex (**1**, black open circle or **2**, blue full circle) with O_2.

originated from a high-spin ferrous species (see Figure S13 for detailed analysis) and can be tentatively assigned as an AsqJ•Fe(II)•succinate•**3** complex. This assignment was corroborated by the observation of an identical quadrupole doublet obtained by a sample containing an anaerobic AsqJ•Fe(II)•**3**•succinate complex (Fig. S11, S13, Table S5). However, this product complex is distinct from the product complex observed in the AsqJ-catalyzed epoxidation reaction[2b] and the product bound TauD complex[9] (Table S4). At 1.5 s, the same enzyme-product complex decreased to ~20%. The lack of accumulation of the Fe(IV)-oxo intermediate suggests that the benzylic H• abstraction is probably not the rate-limiting step under the current experimental conditions.

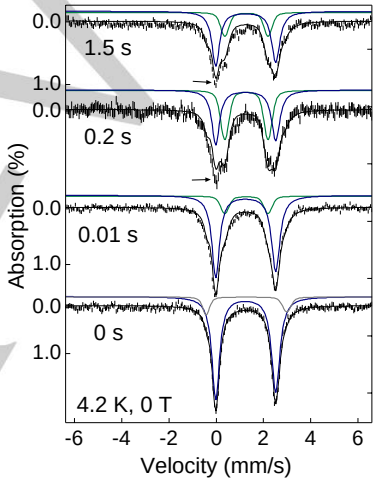

Figure 3. 4.2 K zero-field Mössbauer spectra of the reaction of AsqJ•Fe(II)•2OG•**1** with O_2 at different times. Black vertical bars: experimental data; black lines: overall spectral simulations (*see* Table S2); blue lines: AsqJ•Fe(II)•2OG•**1** complex; green lines: AsqJ•Fe(II)•succinate•**3** complex; grey line: the inactive enzyme (< 10% of the total enzyme). The arrows point to the portion of the spectra at ~0 mm/s that is likely due to the presence of high-spin ferric species by enzyme auto-oxidation (Fig. S12) and is not properly represented by the simulations that only include quadrupole doublets.

To reveal plausible changes to the iron center during the reaction, freeze-quench coupled Mössbauer experiments were performed. The anaerobic AsqJ•Fe(II)•2OG•**1** complex showed a quadrupole doublet with parameters of a high-spin ferrous species (isomer shift δ = 1.25 mm/s and quadrupole splitting $|\Delta E_Q|$ = 2.54 mm/s (Fig. 3, Table S2 and S3). This assignment was validated by the variable field/temperature measurements (Fig. S14, Table S5). The parameters of the AsqJ•Fe(II)•2OG•**1** complex are identical to those of the AsqJ•Fe(II)•2OG•**3** complex (Fig. S11), but are distinct from those of the TauD•Fe(II)•2OG•taurine complex (δ = 1.16 mm/s, $|\Delta E_Q|$ = 2.76 mm/s)[8a]. Compared to the anaerobic sample, the sample quenched at 0.01 s showed ~ 20% consumption of the substrate-AsqJ complex. However, no obvious spectral component representing an Fe(IV)-oxo species was observed. Instead, a new quadrupole doublet, with δ = 1.28 mm/s and $|\Delta E_Q|$ = 1.83 mm/s, developed to ~15% of the total iron (Fig. 3 and Table S2, S3). This species increased to ~30% at 0.2 s with the corresponding decrease of the AsqJ•Fe(II)•2OG•**1** complex to ~40%. This newly formed quadrupole doublet is

Finally, LC-MS analysis was employed to determine the outcome of the AsqJ-catalyzed reaction when **2** was used as a substrate. When the anaerobic AsqJ•Fe(II)•2OG•**2** complex was incubated with excess amount of O_2 for ~20 min, complete consumption of **2** and production of the epoxide (**4**) were observed (similar to the reaction when **1** was used as a substrate). When 2OG was absent, no production of **4** was detected (Fig. 4A and B). This observation implies that **2** is converted to **4** through intermediate **3**, which was previously established for **1**[1]. To establish the production of **3** when **2** was used, chemical quench coupled LC-MS analysis was conducted. LC-MS analysis revealed time-dependent product formation (Fig. 4C). The reaction quenched at 0.2 s showed that **3** was the major product. Subsequently, the sample quenched at 1.5 s showed ~25% increase of **3** production. At 20 s, the amount of **3** decreased and **4** became the major product. Next, the enzymatic assay conducted under limiting 2OG condition revealed that substrate consumption and desaturated product (**3**) formation were at the similar level when either **1** or **2** was tested

10.1002/anie.201710567

(Fig. S16). These results clearly suggest that **1** and **2** are comparable substrates for AsqJ.

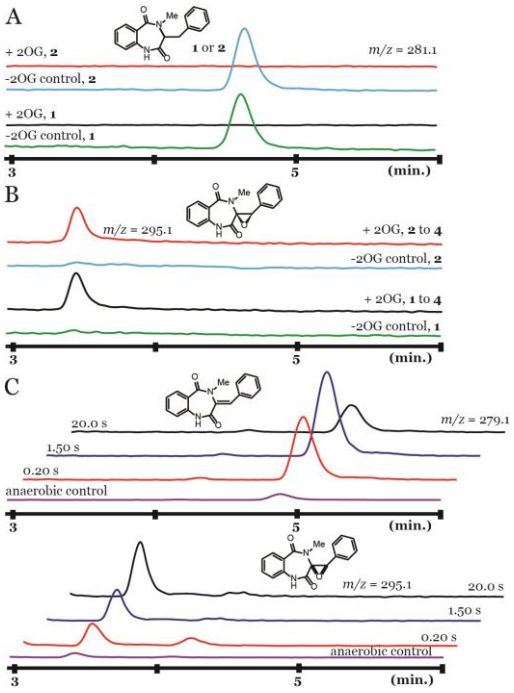

Figure 4. LC-MS chromatogram of AsqJ catalyzed reactions. In panel (A), **1** and **2** were consumed when 2OG was added; (B) **1** and **2** were converted to epoxide **4**; and (C) chemical quench results of **2** at 0.2, 1.5 and 20 seconds and anaerobic control sample revealed the formation of **3** and **4** at different times.

In summary, the experimental data presented herein suggest that both **1** and **2** can be converted to cyclopenin (**4**) through a common intermediate **3** during AsqJ catalysis. Crystallographic structures and MD simulations, together with the SF-Abs, Mössbauer, and LC-MS analyses on the reaction of AsqJ•Fe•2OG•**2** (or **1**) complex reveal that the chirality of C3 is not critical to the desaturation reaction. Furthermore, in the case of **2**, these results suggest that the primary H• abstraction site is at C10 and the subsequent C3-H• abstraction is unlikely due to spatial conformation of **2** in the AsqJ active site. Thus, the AsqJ catalyzed desaturation is likely initiated from C10-H bond activation by a short-lived Fe(IV)-oxo species. Subsequently, a second H• abstraction pathway that has been proposed in P450, di-iron and non-heme iron desaturases[3] is less likely to operate. Instead, pathways involving a carbocation or a hydroxylated intermediate are more likely to be utilized in AsqJ catalyzed desaturation (Scheme 2).

Author Contributions

†These authors contributed equally.

Acknowledgements

This work was supported by North Carolina State University, Carnegie Mellon University, National Taiwan University, and Ministry of Science and Technology grant 106-2113-M-002-021-MY3, R.O.C., Taiwan, We thank Mr. Andrew Weitz and Prof. Michael P. Hendrich for the use of the FQ apparatus. We also thank Mr. Serzhan Sakipov for the MD simulations.

Conflict of Interest

The authors declare no conflict of Interest.

Keywords: desaturation • C-C bond formation • enzyme mechanism • viridicatin • carbocation

[1] N. Ishikawa, H. Tanaka, F. Koyama, H. Noguchi, C. C. Wang, K. Hotta, K. Watanabe, *Angew. Chem. Int. Ed.* **2014**, *53*, 12880-12884.

[2] a) A. Brauer, P. Beck, L. Hintermann, M. Groll, *Angew. Chem. Int. Ed.* **2016**, *55*, 422-426; b) W.-c. Chang, J. Li, J. L. Lee, A. A. Cronican, Y. Guo, *J. Am. Chem. Soc.* **2016**, *138*, 10390-10393.

[3] a) J. L. Abad, F. Camps, G. Fabrias, *Angew. Chem. Int. Ed.* **2000**, *39*, 3279-3281; b) J. L. Abad, F. Camps, G. Fabrias, *J. Am. Chem. Soc.* **2007**, *129*, 15007-15012; c) E. J. Whittle, A. E. Tremblay, P. H. Buist, J. Shanklin, *Proc. Natl. Acad. Sci. U.S.A.* **2008**, *105*, 14738-14743; d) B. Meunier, S. P. de Visser, S. Shaik, *Chem. Rev.* **2004**, *104*, 3947-3980; e) C. A. Reilly, W. J. Ehlhardt, D. A. Jackson, P. Kulanthaivel, A. E. Mutlib, R. J. Espina, D. E. Moody, D. J. Crouch, G. S. Yost, *Chem. Res. Toxicol.* **2003**, *16*, 336-349; f) E. I. Solomon, A. Decker, N. Lehnert, *Proc. Natl. Acad. Sci. U.S.A.* **2003**, *100*, 3589-3594; g) M. Newcomb, R. Shen, S.-Y. Choi, P. H. Toy, P. F. Hollenberg, A. D. N. Vaz, M. J. Coon, *J. Am. Chem. Soc.* **2000**, *122*, 2677-2686; h) L. Britsch, *Arch. Biochem. Biophys.* **1990**, *282*, 152-160; i) J. Zhou, W. L. Kelly, B. O. Bachmann, M. Gunsior, C. A. Townsend, E. I. Solomon, *J. Am. Chem. Soc.* **2001**, *123*, 7388-7398; j) L. Ji, A. S. Faponle, M. G. Quesne, M. A. Sainna, J. Zhang, A. Franke, D. Kumar, R. v. Eldik, W. Liu, S. P. de Visser, *Chem. Eur. J.* **2015**, *21*, 9083-9092; k) R. M. Phelan, C. A. Townsend, *J. Am. Chem. Soc.* **2013**, *135*, 7496-7502. l) D. Usharani, D. Janaradanan, S. Shaik, *J. Am. Chem. Soc.* **2011**, *133*, 176-179; m) H. L. R. Cooper, G. Mishra, X. Huang, M. Pender-Cudlip, R. N. Austin, J. Shanklin, J. T. Groves, *J. Am. Chem. Soc.* **2012**, *134*, 20365-20375.

[4] a) J. M. Bollinger, Jr., W.-c. Chang, M. L. Matthews, R. J. Martinie, A. K. Boal, C. Krebs, Mechanisms of 2-oxoglutarate-dependent oxygenases: the hydroxylation paradigm and beyond. In *2-oxoglutarate-dependent oxygenases*; Hausinger, R. P., Schofield, C. J., Eds.; The Royal Society of Chemistry: London, **2015**, pp. 95-122; b) S. Martinez, R. P. Hausinger, *J. Biol. Chem.* **2015**, *290*, 20702-20711.

[5] a) M. Ishikura, M. Mori, T. Ikeda, M. Terashima, Y. Ban, *J Org Chem* **1982**, *47*, 2456-2461; b) T. Sugimori, T. Okawa, S. Eguchi, A. Kakehi, E. Yashima, Y. Okamoto, *Tetrahedron* **1998**, *54*, 7997-8008.

[6] a) J. Huang, C. S. Li, B. J. Wang, D. A. Sharon, W. Wu, S. Shaik, *ACS Catal.* **2016**, *6*, 2694-2704; b) H. Su, X. Sheng, W. Y. Zhu, G. C. Ma, Y. J. Liu, *ACS Catal.* **2017**, *7*, 5534-5543.

[7] a) E. G. Pavel, J. Zhou, R. W. Busby, M. Gunsior, C. A. Townsend, E. I. Solomon, *J. Am. Chem. Soc.* **1998**, *120*, 743-753; b) J. M. Bollinger, Jr., C. Krebs, *J. Inorg. Biochem.* **2006**, *100*, 586-605.

[8] a) J. C. Price, E. W. Barr, B. Tirupati, J. M. Bollinger, Jr., C. Krebs, *Biochemistry* **2003**, *42*, 7497-7508; b) M. L. Matthews, C. M. Krest, E. W. Barr, F. H. Vaillancourt, C. T. Walsh, M. T. Green, C. Krebs, J. M. Bollinger, *Biochemistry* **2009**, *48*, 4331-4343.

[9] J. C. Price, E. W. Barr, L. M. Hoffart, C. Krebs, J. M. Bollinger, Jr., *Biochemistry* **2005**, *44*, 8138-8147.

10.1002/anie.201710567

WILEY-VCH

COMMUNICATION

An interesting twist in installing a C=C bond was revealed. Desaturation reaction mechanism catalyzed by AsqJ, a non-heme iron enzyme, was elucidated using a complementary approach including probe design, X-ray crystallography, molecular dynamics simulations, and spectroscopic characterizations. Subsequent to the primary C-H bond activation, a carbocation or a hydroxylated intermediate is likely to be involved in the desaturation.

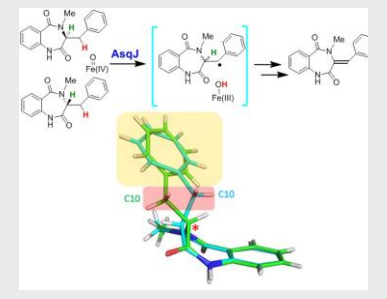

Hsuan-Jen Liao, Jikun Li, Jhih-Liang Huang, Madison Davidson, Igor Kurnikov, Te-Sheng Lin, Justin L. Lee, Maria Kurnikova, Yisong Guo,* Nei-Li Chan,* and Wei-chen Chang**

Page No. – Page No.

Insights into desaturation of cyclopeptin and its C3-epimer catalyzed by a non-heme iron enzyme: structural characterization and mechanism elucidation